168, 1553 (1969).
(4) C. Eon and G. Guichon, *Anal. Chem.*, **46**, 1393 (1974).
(5) J. H. Purnell and J. M. Vargas de Andrade, preceding paper in this issue.
(6) R. L. Scott, *Recl. Trav. Chim. Pay-Bas*, **75**, 787 (1956).
(7) R. Foster, D. Ll. Hammick, and A. A. Wardley, *J. Chem. Soc.*, 3817 (1953).
(8) I. D. Kuntz, F. P. Gasparro, M. D. Johnston, and R. P. Taylor, *J. Am. Chem. Soc.*, **90**, 4778 (1968).
(9) J. Homer, M. H. Everdell, C. J. Jackson, and P. M. Whitney, *J. Chem. Soc. Faraday Trans. 2*, **68**, 874 (1972).
(10) K. Feri and H. J. Bernstein, *J. Chem. Phys.*, **37**, 1891 (1962).
(11) D. E. Martire, *Anal. Chem.*, **46**, 1712 (1974).

Crossed Beam Isotope Labeled Studies of Short-Lived Reaction Intermediates. $CH_3^+ + C_2H_4$

G. P. K. Smith, John Weiner, Martin Saunders, and R. J. Cross, Jr.*

Contribution from the Chemistry Department, Yale University, New Haven, Connecticut 06520.
Received October 11, 1974

Abstract: Crossed beam studies of the ion-molecule reaction $CH_3^+ + C_2H_4 \rightarrow C_2H_3^+ + C_2H_3$ and related isotopic variants involving deuterated and ^{13}C labeled reactants indicate that all products are formed by a direct mechanism, as opposed to a long-lived complex. The ionic products are scattered forward over an energy range of 0.7 to 3.0 eV (CM), with only minor kinematic differences among the various isotopic species. A kinetic model of scrambling and dissociation in a near linear intermediate accounts for the observed relative cross sections of the isotopic products. There is some indication protonated cyclopropane intermediates may play a role at lower energies.

I. Introduction

Carbonium ions represent an important group of reaction intermediates. Our studies of carbonium ion reactions, using beam techniques, provide information on the structure and rearrangements of these ions. Rearrangement in such ions has been studied by NMR and by unimolecular decomposition in mass spectrometers. Two recent reviews are available.[1,2] In addition, some studies of hydrocarbon ion-molecule reactions, involving such intermediates, have been undertaken. These investigations have examined reaction dynamics[3] or isotopic scrambling[4,5] and have focused either on the kinematics of reactive collisions or on the structures of the intermediate species. Our experiments combine these two kinds of information[6] over a range of reaction energies to check the consistency of these two approaches to chemical reactivity and to increase our knowledge of the behavior of this important category of ion-molecule reaction. We report here work on the reaction

$$CH_3^+ + C_2H_4 \longrightarrow C_2H_3 + CH_4 \qquad (1)$$

Extensive research and debate has centered on the structures of $C_3H_7^+$, the intermediate ion in this reaction. Some possible structures for this ion, including a cyclic structure, are shown in Figure 1, with heats of formation given in Table I. Theoretical values are from CNDO calculations of Pople et al.[7]

Using the crossed beam apparatus EVA,[8] we have studied the following variants of reaction 1 at relative (CM) collisional energies from 0.7 to 3.0 eV:

$$^{13}CH_3^+ + C_2H_4 \longrightarrow C_2H_3^+(\text{mass } 27) + {}^{13}CH_4 \qquad (2a)$$

$$\longrightarrow {}^{13}CCH_3^+(28) + CH_4 \qquad (2b)$$

$$CH_3^+ + C_2D_4 \longrightarrow C_2H_3^+(27) + CD_4 \qquad (3a)$$

$$\longrightarrow C_2H_2D^+(28) + CD_3H \qquad (3b)$$

$$\longrightarrow C_2HD_2^+(29) + CD_2H_2 \qquad (3c)$$

$$\longrightarrow C_2D_3^+(30) + CDH_3 \qquad (3d)$$

By measuring the mass, angle, and energy distributions of the products, we have obtained probability contour plots in velocity space indicating the kinematics of the reactions above. In additions, relative cross sections for the different products were calculated[6] at each energy studied.

It is our purpose in this study to determine the extent and pattern of isotopic scrambling in reactions 2 and 3 at various energies; the extent of kinematic differences between different isotopic products; what model or models, if any, involving the intermediate structures in Figure 1 predict the observed isotopic scrambling; and whether the scrambling model is consistent with the kinematics. The model should involve some intramolecular hydrogen migration process for scrambling, in competition with the dissociation of the reaction intermediate to products.

Other experimental work has utilized various $C_3H_7^+$ sources and observed the extent of isotopic scrambling over a wide range of energies and time scales. Saunders et al.[1] have observed scrambling of H and ^{13}C atoms in solutions of isopropyl cation by NMR techniques at 0-40°. They have proposed several possible mechanisms to explain the data including a process required for carbon scrambling involving protonated cyclopropane. Lias, Rebbert, and Ausloos[9] have observed geometrical and isotopic scrambling in $C_3H_7^+$ produced by the radiolysis of *n*-butane and isobutane. The ion cyclotron resonance of McAdoo et al.[10] shows nearly complete hydrogen scrambling in metastable *n*- and *sec*-$C_3H_7^+$ ions produced by electron impact. Nondecomposing *n*-$C_3H_7^+$ ions of lower energy isomerized to *sec*-$C_3H_7^+$, but showed little additional hydrogen scrambling on the ICR time scale ($\sim 10^{-3}$ sec). The present work concerns $C_3H_7^+$ produced by chemical reaction at higher energies and shorter lifetimes than in the previous results.

II. Experimental Section

The apparatus EVA is described in detail elsewhere.[8] Two beam sources are mounted at 90° from each other on a rotatable lid. As the lid is rotated, a detection system scans the angular distributions of products. The ion beam is produced by electron bombardment, mass selected by acceleration into a small permanent magnet, and focused and decelerated to the desired energy by a series of electro-

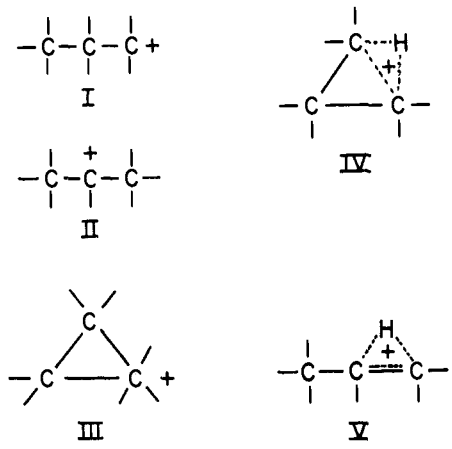

Figure 1. Various proposed structures for the $C_3H_7^+$ intermediate.

static lenses. The neutral beam effuses from a multicapillary source and is mechanically chopped to permit phase-sensitive product detection. Product ions at a given angle are energy analyzed using a retarding potential analyzer and mass selected by a 60° magnetic mass spectrometer, before detection by pulse counting.

Crossed beam experiments on the apparatus EVA were performed for CH_3^+ ion lab energies of 1.0, 2.0, 3.0, and 4.5 eV (relative CM translational energies 0.7, 1.3, 2.0, and 3.0 eV) for reactions 2 and 3. Mass spectra of the products at 3° LAB were also taken for use in calculating total cross sections for the various isotopic products. Ion beams of suitable shape and intensity were unattainable at energies lower than 1.0 eV LAB (0.7 eV CM). Low cross sections and the appearance of significant amounts of isotopically labeled $C_2H_4^+$ and $C_2H_2^+$ products at masses coinciding with those of reactions 2 and 3 prevented work at energies higher than 4.5 eV LAB (3.0 eV CM). The $^{13}CH_3^+$ contained approximately 7% $^{12}CH_4^+$. This impurity, however, produced less than 1% of the total product intensity in the mass region under investigation and could be ignored.

The isotopic studies are complicated by the occurrence of the following slightly endothermic ($\Delta H = -0.59$ eV[11]) reactions. The

$$CH_3^+ + C_2H_4 \longrightarrow C_2H_4^+ + CH_3 \quad (4)$$

$$^{13}CH_3^+ + C_2H_4 \longrightarrow C_2H_4^+(\text{mass } 28) + {}^{13}CH_3 \quad (5a)$$

$$\longrightarrow {}^{13}CCH_4^+(29) + CH_3 \quad (5b)$$

$$CH_3^+ + C_2D_4 \longrightarrow C_2H_3D^+(29) + CD_3 \quad (6a)$$

$$\longrightarrow C_2H_2D_2^+(30) + CD_2H \quad (6b)$$

$$\longrightarrow C_2HD_3^+(31) + CDH_2 \quad (6c)$$

$$\longrightarrow C_2D_4^+(32) + CH_3 \quad (6d)$$

cross section for reaction 4 varies from 3 to 10% of that for reaction 1 over the energy range studied. Our results show the kinematics of reactions 1 and 4 are similar, and that isotopic scrambling takes place in reactions 5 and 6 as well. Thus the mass 28 peak from ^{13}C labeling work on reaction 2 is a mixture of reactions 2b and 5a. Similarly, for reaction 3, products 3c and 6a, as well as 3d and 6b, coincide at mass 29 and 30, respectively. Corrections for the flux due to reactions 5a, 6a, and 6b were made in calculating relative cross sections.

The method for calculating relative cross sections for reactions 2 and 3 follows. First, the cross section for reaction 4 relative to reaction 1 was determined. This involved integrating over the probability contour plots to determine the total flux produced relative to that measured at 3° LAB for each product. A full discussion of this procedure may be found elsewhere.[6] For reactions 2 and 5 a similar procedure was followed to obtain relative cross sections for the products of mass 27 (eq 2a), mass 28 (eq 2b and eq 5a), and mass 29 (eq 5b). The difference between the relative cross sections for reaction 4 and 5b is roughly the relative cross section for reaction 5a. The relative cross section for reaction 2b is just the difference between those for mass 28 and reaction 5a. The procedure for

Table I. Heats of Formation (kcal/mol) of Various $C_3H_7^+$ Configurations

Figure 1 structure	System	ΔH_f^{EXP}	$\Delta H_f^{TH(?)}$	$-\Delta H_r$
	$CH_3^+ + C_2H_4$	273[11]		
	$C_2H_3^+ + CH_4$	251[11]		22
	$C_2H_4^+ + CH_3$	287[11]		−14
I	n-$C_3H_7^+$	208[12]	206	65
II	sec-$C_3H_7^+$	192[12]	(192)	81
III	Corner c$C_3H_7^+$	200[13]	205	73
IV	Edge c-$C_3H_7^+$		211	62
V	H bridged n-$C_3H_7^+$		203	70

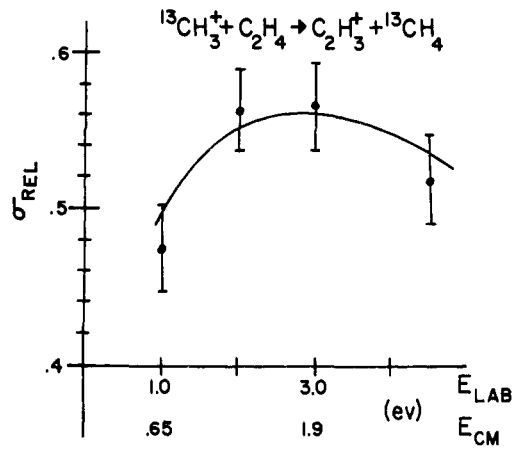

Figure 2. Relative cross section for reaction 2a vs. ion energy (LAB and CM).

reaction 3 was complicated by the existence of two such ambiguous masses (29, 30) preventing the exact correction technique employed above. The reaction 4 intensity not observed directly as (6c) or (6d) was divided equally between (6a) and (6b). The additional uncertainty introduced into the calculation of relative cross sections for reactions 3c and 3d by this method or by isotope effects on reaction 4 cross sections was included in the estimation of probable error. In many of the above determinations, the cross sections for isotopically labeled reaction 4 processes were too small to allow the construction of contour plots. In light of past experience, it is reasonable to assume contour plots similar to the unlabeled reaction 4 result. The error possibly introduced by this difficulty into the relative cross sections for reactions 2 and 3 is minor.

III. Results

Ratios of cross sections for reaction 2 are shown in Figure 2, a plot of $\sigma(2a)/[\sigma(2a) + \sigma(2b)]$ vs. relative collisional energy. While the unlabeled product of (2a) is roughly 50% at all energies, a trend to lower percentages at high and particularly low energies is apparent. Figure 3 is a similar plot for reaction 3. At low energies, very marked changes in the distribution of products occur. The product of (3c), $C_2HD_2^+$, increases while that of (3d), $C_2D_3^+$, drops. The complimentary trends are shown in Figure 4 for the reverse isotopic system, $CD_3^+ + C_2H_4$. Minor differences between the two systems are attributable to experimental inaccuracy, differences in primary ion internal energy, and possible isotope effects.

Since, to our knowledge, no previous measurements of the total cross section for reaction 1 have been made, we attempted some rough estimates. Because the determination of the total reactant and product fluxes is very difficult with an apparatus such as EVA, these values have order of magnitude accuracy only, and serve to illustrate the general decline of the cross section at higher energies. Results are shown in Table II. The cross section for reaction 4 was 3 to 4% of reaction 1 at the lower energies, but jumped to 7% at 4.5 eV (LAB). Operation of the source at high electron cur-

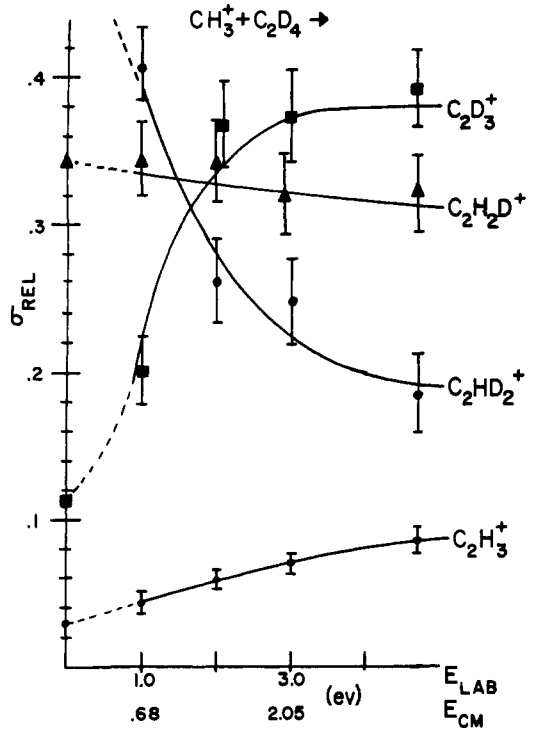

Figure 3. Relative cross sections for reactions 3a, 3b, 3c, and 3d.

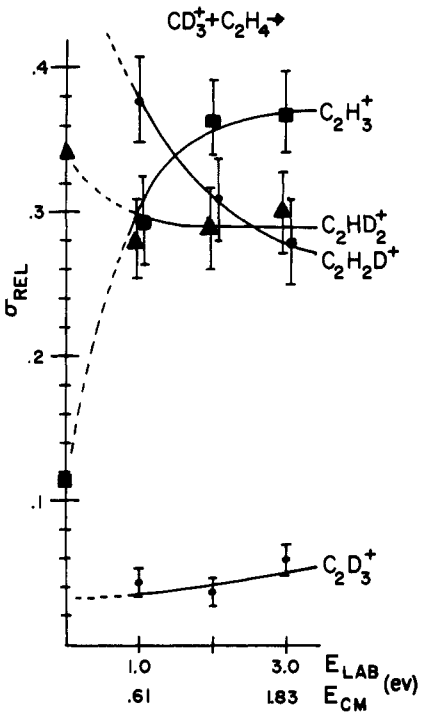

Figure 4. Relative cross sections for the isotopic complement of reaction 3, $CD_3^+ + C_2H_4$.

Table II. Reaction 1 Cross Section vs. Ion Energy

E_{LAB}, eV	1	2	3	4.5
σ_1, Å^2	12	8	2.5	.6

Table III. Effects of Internal CH_3^+ Energy

E_{REL}, eV		$\sigma(4)/\sigma(1)$	Q_1, eV	Q_4, eV
0.7	CH_3^+	0.03	−0.02	
	CH_3^{+*}	0.07	+0.68	+0.16
1.3	CH_3^+	0.04	−0.32	−0.20
	CH_3^{+*}	0.11	+0.25	+0.05
Q_{MAX}			+0.95	−0.59

rents, however, produced a marked increase in the cross section for reaction 4, particularly at lower energies as shown in Table III.

Source conditions also had a sizable effect on the energy distributions of the products. Table III gives the Q values, the difference between the most probable relative (CM) translational energy of the products and that of the reactants. A more positive Q value indicates the product ion has more translational energy. Q_{MAX} is the largest value allowed by the enthalpy of reaction for reactant ions having no internal energy. For both reactions 1 and 4, the high electron current source conditions produced products with more translational energy. The Q values for reaction 4 exceed Q_{MAX} and indicate that the CH_3^+ reactant ions in the majority of reactive collisions have considerable internal energy (~0.75 eV). We thus conclude that the altered source conditions produced a greater proportion of internally excited CH_3^+ ions, which enhance the cross section for reaction 4 and increase the product translational energy for reactions 1 and 4. The charge-transfer studies of Tal'roze et al.[14] for CH_3^+ and various gases indicate that both electronically and vibrationally excited CH_3^+ may be produced in our source, but his lifetime estimate of 5×10^{-7} sec for the electronically excited state present is much less than the transit time for our ions to the collision region. The substantial variation in the peak product energy observed for reaction 1 indicates that any small observed differences in product kinematics for reactions 2a and 2b and 3a-d might be due to changing source conditions affecting the distribution of vibrational excitation in the primary beam. This brief investigation indicates the possible effects of reactant vibration on kinematics and points out the need to control carefully the source conditions for all aspects of experiments on this particular reaction.

The probability contour plots[15] for reactions 2 and 3 at 2 eV LAB energy are presented in Figures 5 and 6, respectively, and are typical of results at other energies. Results confirm a direct mechanism with predominantly forward scattering and no major differences among the various products. None of our data show evidence for a backscattered peak, and the point beyond which no further backscattered ions were detected is still well within the angular range (50° LAB) and energy range (0.1 eV LAB) of the apparatus. Since no persistent complex is formed, as evident by the product anisotropy with respect to the center of mass, the intermediate or intermediates live on the average less than a rotational period (10^{-12} sec).[16] A few minor kinematic differences were observed. Reaction 2a product was slightly farther forward than (2b). Also, Q values for reaction 3c were lowest and for reaction 3d were highest (least internal excitation in products) for most experiments on reaction 3.

IV. Discussion of Mechanisms

A complete description of the reactions involves the knowledge of all classical trajectories (or the complete wave function). With ten atoms all interacting strongly, we cannot approach this much detail. Nevertheless, it is possible to devise some simple models for the various isotopic rearrangements. Our simplest models, referred to as "static", contain no kinematic information; they predict only the relative cross sections for the various isotopic products. The reactants are assumed to form a short-lived intermediate "complex" which may then rearrange or it may dissociate to form the products. This sort of model is more appropriate to a long-lived complex than the present case, but because of the simplicity of the models we can test them easily. Our

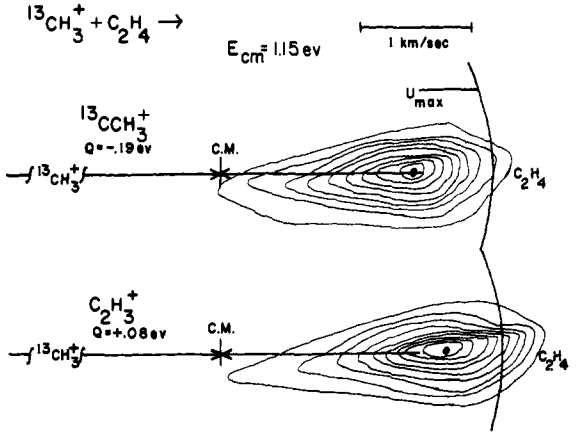

Figure 5. Product intensity contour plots in a Cartesian velocity space[14] for reactions 2a and 2b at relative energy of 1.15 eV (CM). Each plot is separately normalized, and contours are drawn at 10% intensity intervals. The center line is a portion of the relative velocity vector, and the forward arc is the maximum product velocity permitted from unexcited reactants by the reaction exothermicity. Note the greater forward scattering for reaction 2a.

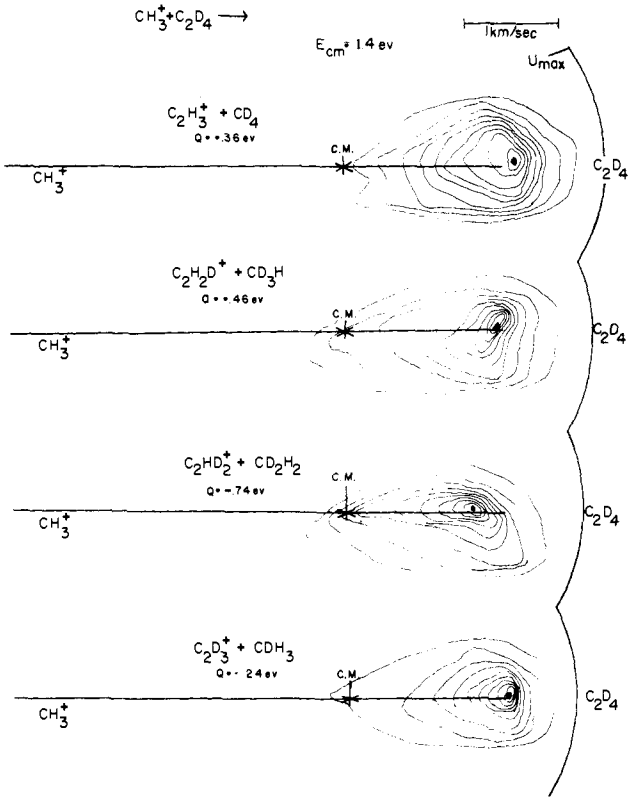

Figure 6. Similar product intensity contour plots for reactions 3a, 3b, 3c, and 3d at E_r = 1.40 eV. Note the product of (3c) is less forward scattered than the others, a trend also seen at other energies.

preferred candidate, linear model I, presumably bears some relation to the full reaction dynamics.

The static models involve rearrangements between several isomers of an assumed "complex". If isotope effects are neglected, the rearrangements of the "complex" involve only one or two rate constants. In competition with the rearrangements is the dissociation to products. The product isotopic ratios are simply obtained as the solution of several compled linear rate equations. In the simplest cases the relative yields of the several products are determined by a single ratio of rate constants. Different models, of course, give different product ratios. First, we discuss three simple models and a fourth, somewhat more complicated, one which at-

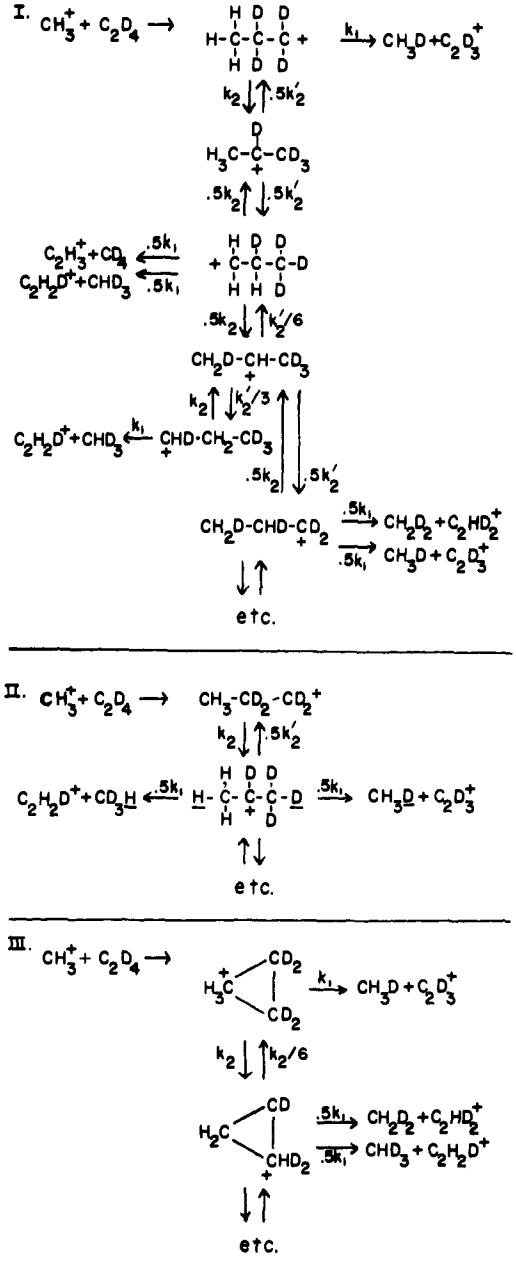

Figure 7. The three simple proposed scrambling and dissociation schemes for reaction 1.

tempts to explain some of the kinematics. Next, we discuss the implications of combining two or more of these models. These simple static models do not give any predictions of the angular distributions. The reaction dynamics of these systems do not lend themselves to any simple interpretation. The final section is a brief discussion of more complicated dynamic models.

Static Models. The four simplest models for scrambling and dissociation among possible reaction 1 intermediates are presented in Figures 7 and 8. More complicated models will be considered briefly later. Linear model I (Figure 7) scrambles the hydrogens and the end carbons by a series of *n*-propyl ion to *sec*-propyl ion isomerizations. The transition state for this process is structure V of Figure 1. The competing dissociation to products involves the abstraction of a neighboring hydrogen atom by the departing methyl group. The ratio of various isotopic products predicted by this model depends only on the ratio k_1/k_2 and is independent of k_2'.

Linear model II (Figure 7) involves the same scrambling scheme, but dissociation occurs from the *sec*-propyl struc-

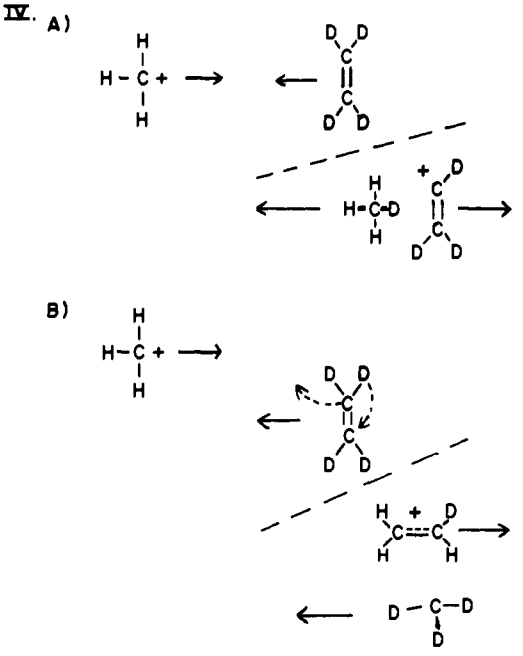

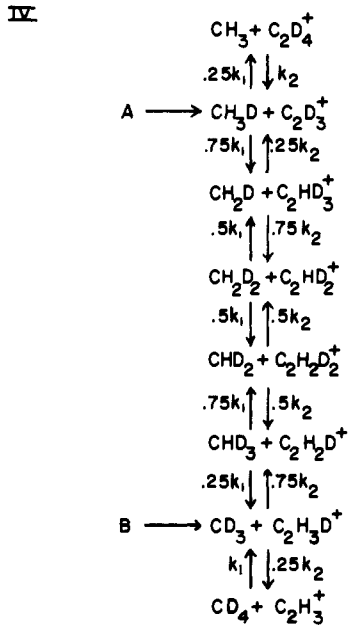

Figure 8. The fourth scrambling scheme for reaction 1, including initiation steps A and B.

ture. Here the departing neutral methyl abstracts a hydrogen from the opposite end of the intermediate ion. Although this seems less likely than the dissociation step of model I from the primary ion intermediates, it must be considered since the time spent in the lower energy *sec*-propyl structure is probably greater.[9] The predictions of model II depend only on k_1/k_2' and are independent of k_2.

Ring model III (Figure 7) considers a protonated cyclopropane structure for the intermediates. Similar structures have been considered as intermediates of other ion-molecule reactions.[5] The transition state for scrambling is the edge protonated form IV of Figure 1. The dissociation step is CH_3^+ abstracting an H^- from either of the equivalent neighboring CH_2 groups. This predicts the same results as a ring-opening step to an *n*-propyl ion and subsequent decomposition similar to model I, without additional scrambling.

Model IV, shown in Figure 8, begins with two separate mechanisms for forming the initial intermediate. For reac-

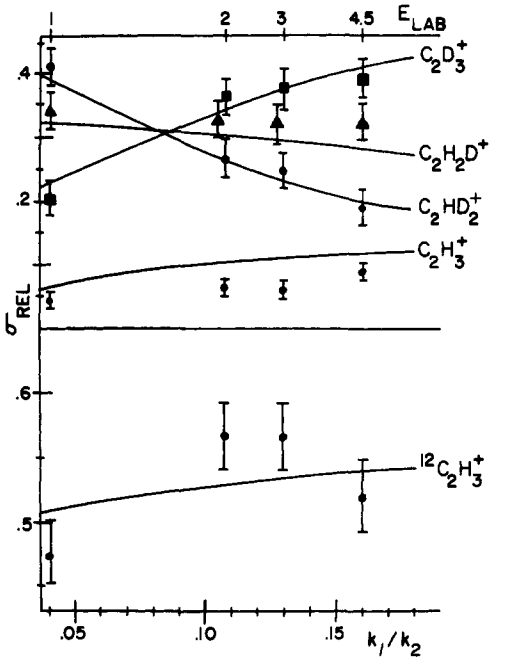

Figure 9. The predictions of model I for the relative cross sections of reactions 2 and 3 as a function of the ratio of dissociation rate to scrambling rate. For comparison, experimental points have been included, positioning reaction 3 data for the best fit to the theoretical curves.

tion 3, trajectories following path A involve abstraction of D^- from C_2D_4 by CH_3^+. Path B involves CD abstraction by CH_3^+ from C_2D_4. Scrambling of the hydrogen atoms then occurs by H or D atom jumps, from CX_4 to $C_2X_3^+$ and from $C_2X_4^+$ to CX_3 (X = H, D). Note that for ^{13}C labeling (reaction 2, $^{13}CH_3^+ + C_2H_4$), the ratio of products depends only on the ratio of rates for paths A and B. Path A produces only unlabeled ion products, $C_2H_3^+$ (reaction 2a), while path B produces only labeled $^{13}CCH_3^+$ (reaction 2b), so the scrambling scheme never rearranges carbon atoms. The $C_2H_4^+ + CH_3$ configuration is probably the point of highest energy in this scheme. The model IV predictions for reaction 3 ($CH_3^+ + C_2D_4$) depend on the ratio A/B, empirically determined from the data for reaction 2, and on the time allotted for scrambling. After this time t, the products have receded too far to allow further H migrations. The ratio k_1/k_2 only determines the ratio of $C_2H_3^+$ products (reaction 1) to the $C_2H_4^+$ products (reaction 4) also predicted by this model.

Assuming, for the moment, that such a scheme, as outlined above, for scrambling among intermediates in competition with dissociation is a valid procedure for describing the reaction, we will examine the predictions of the various models. Comparison with the experimental relative cross sections for reactions 2 and 3 should then yield some information on the intermediate structures for reactive collisions in this system. The predictions were obtained by determining the proper rate equations for the various intermediate and product isomers involved in a given model and solving these equations by numerical integration techniques or an alternate matrix method.[6] Figures 9–12 show the results for models I, II, III, and IV, respectively. The data points have been inserted for comparison, and the best fit of the reaction 3 data was used to determine the correspondence between collision energy and the theoretical rate ratio. Note that this system is reactive, and our $C_3H_7^+$, in contrast to that of Lias et al.,[9] has sufficient energy to dissociate. Thus the effect of increased energy is to shorten the time of collision for a direct process,[6] speeding up dissociation of the in-

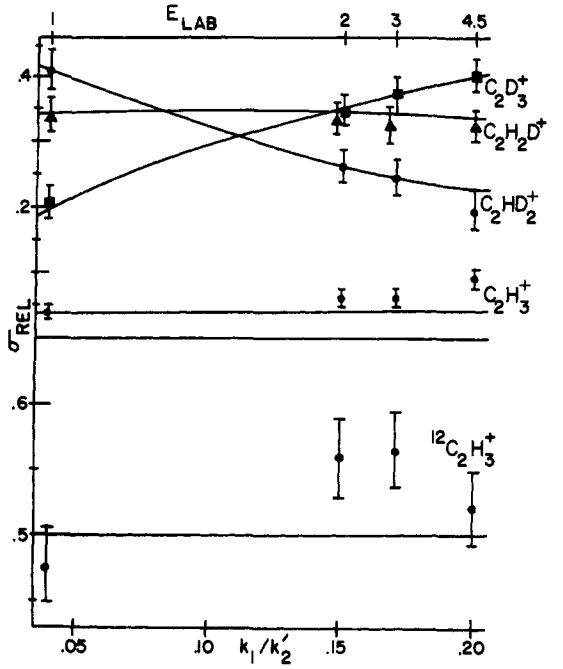

Figure 10. Predictions of theory II, similar to Figure 9.

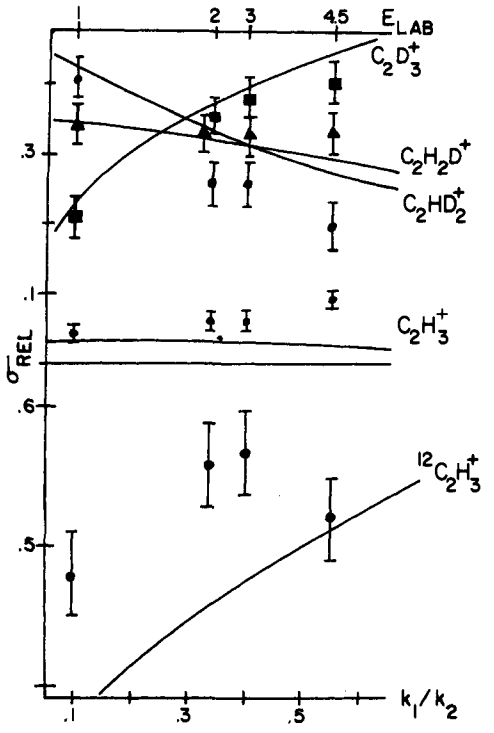

Figure 11. Predictions of theory III, the ring model, similar to Figure 9.

termediates as reflected in the increase of k_1/k_2 with E in Figure 9.

Examination of Figures 9 and 10 reveals that both linear models I and II fit the observed relative cross section data satisfactorily. The fits of both models to the reaction 2 data are not as good. While neither model predicts the apparent high-energy decrease in the reaction 2a percentage, model I does qualitatively predict the drop at low energies.

The ring model, as shown in Figure 2, clearly fails to match the experimental results. This is particularly apparent for the high-energy data on reaction 3 and the entire data on reaction 2. Note, however, that the lowest energy percentage for reaction 2a is below the 50% random scrambling lower limit for linear models. The corresponding value

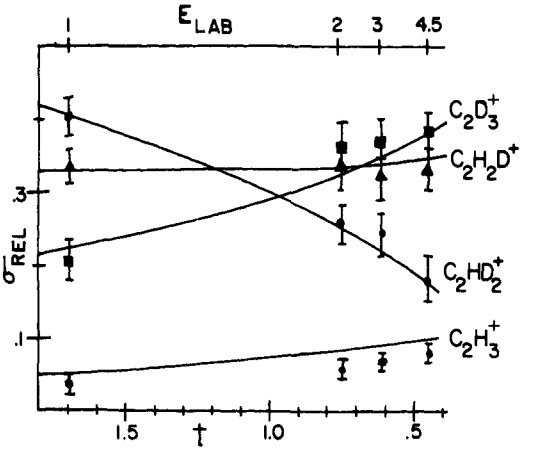

Figure 12. Predictions of theory IV, similar to Figure 9.

for the ring model is 33%. Should this trend below 50% persist at lower energies than we could attain, it would be evidence for the participation of ring intermediates in the reaction at low energies. Thermal ICR experiments, complementary to ours, may decide this issue.

If two or more mechanisms are occurring at the same time, it is highly likely that the ratio of rates for the two mechanisms would vary with energy. The cyclic mechanisms may be more probable at lower energies.

Model IV also fits the data for reaction 3 satisfactorily, as shown in Figure 12. Note that at higher energies the time for scrambling is shorter, reflecting the shorter time of a collision event at higher velocities. Unfortunately, this model can make no predictions for reaction 2, since the ratio of rates for A/B is synonymous with the ratio of cross sections for (2a)/(2b). The inability of models I and II to fit the data of reaction 2 precisely, however, indicates the two-mechanism approach used in model IV cannot be ruled out.

An attempt was made to determine clearly which of the models I, II, or IV is primarily responsible for the reaction. The models predict distinctly different ratios at high energies for the two major production masses of reaction 7. The

$$^{13}CH_3^+ + C_2D_4 \longrightarrow C_2D_2H^+ + {}^{13}CD_2H_2$$

or

$$^{13}CCDH_2^+ + CD_3H \qquad (7a)$$

$$\longrightarrow C_2D_3^+ + {}^{13}CDH_3$$

or

$$^{13}CCD_2H^+ + CD_2H_2 \qquad (7b)$$

rate ratios used to determine theoretical predictions of (7a)/(7b) are indicated by the match of experimental data to the models in Figures 9, 10, and 12. Model and experimental results shown in Table IV support the use of linear model I over model II or IV to describe the reaction at high energy. At low energy, however, neither model provides a satisfactory fit. This may indicate a more complicated process is occurring.

It is perhaps worth noting that the preferred model, linear model I, is intuitively the scrambling scheme one might expect. It provides the lowest energy pathway for isotopic scrambling, especially as compared to model IV. Perhaps more important, in view of the large energies available in these experiments, this path is also the most favored by what one might term *entropy factors*. Models II and III have at least one step which requires a rather specific arrangement of the carbon atoms, either in a ring for ring scrambling (model III scrambling) or a near-ring bent structure for a 1,3 hydrogen shift (model II dissociation).

Table IV. Ratio of Cross Sections for Reaction $\sigma(7b)/\sigma(7a)$

E_{LAB}	2.0	4.5
EXP	1.2	1.2
TH1	1.0	1.2
TH2	0.6	0.6
TH4	0.8	0.9

The high-energy reaction intermediate will likely spend little time in these particular configurations in view of the many other energetically available ones, and hence the rates for ring scrambling and 1,3 shifts will be low.

In contrast to the NMR results of Saunders et al.,[1] our experiments indicate little scrambling via protonated cyclopropane intermediates. Our work, however, involves much higher energies, very short-lived $C_3H_7^+$ ions formed in the course of a chemical reaction, and gas phase work rather than solution. Yet we do see some low-energy evidence in reaction 2 for the participation of protonated cyclopropane intermediates, and lower energy relative cross sections by other techniques, perhaps ICR, would be useful.

The results of Lias et al.[9] on $C_3H_7^+$ rearrangements in the gas phase radiolysis of butane and isobutane provide another interesting comparison. They found that certain of the *n*-propyl ions (structure I) underwent ring closure and tended to retain this structure while rapidly scrambling hydrogens. This effect was smaller at high energies, and our reaction apparently shows little of this behavior. Their results also show significant energy-dependent hydrogen scrambling, and with the work of McAdoo et al.[10] indicate $C_3H_7^+$ spent more of its time in structure II than I.

More complicated models and combinations were also examined, although the use of additional processes usually precluded an unambiguous fit between sets of rate constants and the data. Several combinations of models I and II, permitting dissociation from both *n*- and *sec*-propyl intermediates, will also work. Some additional scrambling of *sec*-propyl intermediates through 1,3-hydride shifts is also consistent. However, since this process alone would produce no $C_2H_3^+$ (reaction 3a), the rate for the normal linear scrambling process must exceed the 1,3-shift rate. A final possible mechanism involves limited scrambling in the ring intermediates before opening to the *n*-propyl form and subsequent linear scrambling. This combination of model III with I and/or II would be consistent with the low-energy reaction 2 behavior discussed previously. The data fit this scheme well only when ring dissociation to the linear form is much faster than ring scrambling; i.e., most scrambling takes place in the linear form. Addition of a significant rate for ring closure, a process not favored in energy or entropy, gave very poor results. Finally, the addition of a simple, direct, independent H^- abstraction channel by the reactant CH_3^+ ions (producing the products in reactions 2a and 3d) to the other models also failed.

Dynamic Models. One final problem to be considered concerns the validity of any scrambling model. This reaction occurs for a large set of different trajectories, each of which can be viewed as a succession of different $C_3H_7^+$ intermediates. Our static model for this collection of dynamic processes is thus a very severe limitation on the number of intermediates considered. Any success for such a model can only be considered a rough indication of the likely atomic motions during an average collision, a crude model for the average of dynamic pathways. The poor fit of the model for reaction 2 and reaction 5 at 2 eV indicates that processes much more complex than those we considered may be occurring.

The consistency of the scrambling model and the dynamics sheds further light on the problem. Consider the time scales involved. We estimate the time for hydrogen transfer (scrambling) is roughly 10^{-14} sec (one vibration) from considering propylene vibrational frequencies.[17] An estimate of the rotational period of the intermediate from the rough cross section data[18] indicates that roughly 40 vibrations occur during one such rotation at 1 eV LAB energy. Linear model I predicts the rate for scrambling at this energy is 25 times that for dissociation, leading to a predicted half-life for the complex of 0.4 rotations. If this were the case, a fair amount of backward scattered ion products would be observed at 1 eV. Either the hydrogen transfer is much faster than expected, the impact parameter of the average reactive collision is much larger than expected (2.5 Å) thus increasing the rotational period, or the model presented is incorrect despite its apparent success in predicting relative isotopic cross sections.

Considerable backscattering of product ions relative to the center of mass also would have resulted from any carbon atom "forgetting" its original direction of motion. In no event does the scrambling process scramble the motions of the various carbon nuclei. The potential surface for this reaction cannot allow the momenta of the various carbon atoms to randomize to any appreciable extent.

The nearly identical kinematics for all products present another challenge to structural models. All ionic products at all energies are almost entirely forward scattered, and show similar peaks and distributions. This occurs despite the differing degrees to which the average precursors of the different products have undergone scrambling. The similarity of the kinematics implies that the scrambling process has little effect on the partitioning of the energy between translation and internal modes. Neither the original momenta of the various hydrogen atoms nor the extent to which they scramble has much net effect on the final product distribution. The nearly identical kinematics also appear independent of whether or not the product ion incorporates the carbon atom of the CH_3^+ reactant. For model I, one intuitively expects the direction of the CX_4 neutral to alternate, depending on which end of the intermediate the departing CX_3 group originated. Yet there is no evidence for such a forward-backward pattern in the probability contour plots. In reaction 2a, the labeled ^{13}C atom in the reactant ion recoils backward as the neutral product, while in reaction 2b it continues forward as part of the ion product.

The simple linear model I accounts for the above reversal of ^{13}C atom momentum as the result of transferring a H atom by the scrambling scheme from one end carbon atom to the other. The carbon atom on which the positive charge is centered when dissociation of the intermediate occurs must move forward. The hydrogen migrations which effectively move this charge must also reverse the motions of the carbon atoms. It is difficult to visualize such a dramatic dynamic effect as the result of simple hydrogen atom jumps, although such events may well occur. The product distributions require a high degree of correlation between the motion of each carbon atom and the hydrogen scrambling process. In this scheme, the final motions of the carbon atoms are determined only after the final scrambling step. The scrambling and exit regions of the potential surface are separate.

In an alternate view of the reaction, the dynamics and hydrogen scrambling are uncoupled, and the dynamics are predetermined by the initial trajectory of the reactants. Consider the following modification of model I. For certain trajectories, say most nearly head-on, the ^{13}C rebounds, and must be part of the neutral methane product. Only the dissociations to the right in Figure 7-I are permitted from the various scrambling intermediates. There is a kinematic or potential barrier to other dissociations (those to the left).

For other trajectories, the $^{13}CH_3^+$ strips a C from the C_2H_4, and only dissociations to the left are allowed. This model envisions a potential surface of two reaction paths with very similar scrambling and energy partioning features. It is also similar to model IV in using reaction 2 data for the theory rather than using the theory to fit the reaction 2 data. The closeness of the original model I fit to the reaction 2 data, however, means the revised model outlined here has no significant effect on the predicted cross sections for reactions 3 and 5.

Of the two model I mechanisms, the revised version just presented rests upon the more reasonable assumptions. The existence of two mechanisms with similar net results seems more likely than the reversal of C atom momenta with each proton jump. Yet, without the experimental kinematic information, the original static version of model I would have been acceptable and simpler. This reaction thus illustrates the importance of examining the experimental reaction dynamics when considering simplified models for a reaction, and warns of the danger of viewing a reactive event in terms of static intermediates.

V. Conclusions

1. The reaction takes place via a direct mechanism, although considerable C and H scrambling occurs. All ionic products are predominantly formed forward of the center of mass.

2. In our energy range, the isotopic scrambling can be accounted for by a simple model involving linear intermediates.

3. Despite any scrambling processes, or the likelihood of two separate mechanisms, the kinematics of all products are similar. This behavior is more clearly illustrated by reaction 1 than the previously studied methyl cation–methane reaction,[19] but may prove typical for many reactions in which scrambling occurs. Experiments on other carbonium ion reactions are in progress. In addition, theoretical trajectory studies of this or similar reactions,[20] while difficult, might clarify the puzzling behavior of this system.

Acknowledgment. Research support from the National Aeronautics and Space Administration is gratefully acknowledged.

References and Notes

(1) M. Saunders, P. Vogel, E. L. Hagen, and J. Rosenfeld, *Acc. Chem. Res.*, **6**, 53 (1973).
(2) J. T. Bursey, M. M. Bursey, and D. G. I. Kingston, *Chem. Rev.*, **73**, 191 (1973).
(3) Z. Herman, A. Lee, and R. Wolfgang, *J. Chem. Phys.*, **51**, 452 (1969); Z. Herman, P. Hierl, A. Lee, and R. Wolfgang, *ibid.*, **51**, 454 (1969); A. Ding, A. Henglein, and K. Lacmann, *Z. Naturforsch., Teil A*, **23**, 2084 (1968).
(4) W. T. Huntress, Jr., *J. Chem. Phys.*, **56**, 5111 (1972); T. O. Tiernan and J. H. Futrell, *J. Phys. Chem.* **72**, 3080 (1968).
(5) J. Weiner, A. Lee, and R. Wolfgang, *Chem. Phys. Lett.*, **13**, 613 (1972).
(6) J. Weiner, G. P. K. Smith, M. Saunders, and R. J. Cross, Jr., *J. Am. Chem. Soc.*, **95**, 4115 (1973).
(7) P. C. Hariharan, L. Radom, J. A. Pople, and P. v. R. Schleyer, *J. Am. Chem. Soc.*, **96**, 599 (1974); L. Radom, J. A. Pople, V. Buss, and P. v. R. Schleyer, *ibid.*, **94**, 311 (1972).
(8) Z. Herman, J. D. Kerstetter, T. L. Rose, and R. Wolfgang, *Rev. Sci. Instrum.*, **40**, 538 (1969).
(9) S. G. Lias, R. E. Rebbert, and P. Ausloos, *J. Am Soc.*, **92**, 22 (1970).
(10) D. J. McAdoo, F. W. McLafferty, and P. F. Bente III, *J. Am. Chem. Soc.*, **94**, 6 (1972).
(11) J. L. Franklin, J. G. Dillard, H. M. Rosenstock, J. T. Herron, K. Draxl, and F. H. Field, *Natl. Stand. Ref. Data Ser., Natl. Bur. Stand.*, **No. 26** (1969).
(12) F. P. Lossing and G. P. Semeluk, *Can. J. Chem.*, **48**, 955 (1970).
(13) S.-L. Chong and J. L. Franklin, *J. Am. Chem. Soc.*, 634 (1972).
(14) N. V. Kir'yakov, M. I. Markin, and V. L. Tal'roze, *Vys. Energ.*, **7**, 94 (1973); 178 (1973).
(15) R. Wolfgang and R. J. Cross Jr., *J. Phys. Chem.*, **73**, 7[illegible] (1969).
(16) W. B. Miller, S. A. Safron, and D. R. Herschbach, *Discuss. Faraday Soc.*, **44**, 108 (1967).
(17) R. C. Lord and P. Venkateswarlu, *J. Opt. Soc. Am.*, **43**, 1079 (1953).
(18) The rotational period can be calculated from the angular momentum, estimated by $L = \mu bg$ where μ is the reduced mass of the colliding reactants, g is the relative collisional velocity, and b is the maximum impact parameter leading to reaction, estimated from the cross section by $b = (\sigma/\pi)^{1/2}$. Then $\tau = 2\pi I/L$ where $I \approx \frac{1}{2}\mu b^2$.
(19) Consider the reaction of ref 5, $CH_3^+ + CH_4 \rightarrow C_2X_5^+ + X_2$, in which the majority of all isotopic ion products are forward scattered. This occurs regardless of the end of the $C_2H_7^+$ complex from which the X_2 dissociates.
(20) R. Hoffmann, D. M. Hayess, and P. S. Skell, *J. Phys. Chem.*, **76**, 664 (1972), have done some calculations of the isoelectronic $CH_2 + C_2H_4$ surface.

Gaseous Ionic Acetylation of Cresols

Dale A. Chatfield[1] and Maurice M. Bursey*[2]

Contribution from the Venable and Kenan Chemical Laboratories, The University of North Carolina, Chapel Hill, North Carolina 27514. *Received October 4, 1974*

Abstract: Rates of the ion–molecule reaction of *o*-, *m*-, and *p*-cresol with $CH_3COCO(COCH_3)CH_3^+$, $CH_3CO{\cdot}(COCH_3)CH_3^+$, and CH_3CO^+ were measured by ion cyclotron resonance and compared with calculated results. The relative insensitivity of the rate to the choice of neutral isomer was duplicated, but only modest agreement was found on examining sensitivity to the choice of ionic acetylating species.

There have been several approaches to the study of reactions resembling electrophilic aromatic substitutions in the gas phase. One approach has been through the ion cyclotron resonance technique.[3-5] The other has been through high-energy ion chemistry.[6-8] In addition, the acylation of oxygen-containing compounds has been studied by ion cyclotron resonance with the use of a variety of precursors.[9,10]

In connection with these studies, and in an attempt to explore the applicability of accepted theories of ion–molecule reaction rates to very complex organic reactions, we have now studied the rates of acetylation of the three isomeric cresols using two different precursors of the acetyl ion, acetone and biacetyl. Conventional ion cyclotron resonance (ICR) techniques were used.

Experimental Section

A Varian V-5900 ICR spectrometer was used for all experiments. It was equipped with a standard (1.27 × 2.54 × 14 cm)